Solid Freeform Fabrication 2022: Proceedings of the 33rd Annual International Solid Freeform Fabrication Symposium – An Additive Manufacturing Conference
Reviewed Paper

GENERATION AND ANALYSIS OF ALSI10MG L-PBF SINGLE TRACK DATA SET ENABLING DEEPER PROCESS INSIGHTS

Conor Porter[1], Fred Carter[1,2], Dominik Kozjek[1], Andrea Cardona[3], Jon-Erik Mogonye[4], Kornel Ehmann[1], and Jian Cao[1]

[1]Department of Mechanical Engineering, Northwestern University, Evanston, IL 60208, USA
[2]DMG MORI Advanced Solutions Inc., Hoffman Estates, IL 60192, USA
[3]Department of Materials Science and Engineering, Northwestern University, Evanston, IL 60208, USA
[4] U.S. Army DEVCOM Army Research Laboratory, Aberdeen Proving Ground, MD 21005, USA

Abstract

The stability of the melt pool in Laser Powder Bed Fusion (L-PBF), especially with process perturbations, is a key factor underpinning the success of additively manufactured components. In metal Additive Manufacturing (AM), single tracks are widely used to verify and validate simulation and process models. This work describes the creation of a holistic L-PBF single track data set incorporating a large domain of process conditions for AlSi10Mg. The 352 single tracks are characterized through a series of high throughput methods including white light interferometry, automated microstructure analysis, and in-situ high-frequency (up to 200 kHz) coaxial melt pool monitoring. This data constitutes a large database of process parameters, high-resolution measurements, and geometry information for data driven analysis, including machine learning. In one approach this data is used to correlate track shape and melt pool characteristics to in-situ measurements.

Introduction

The success of the L-PBF process can be distilled to the stability and reliability of the melt pool process. There is significant research in micro- and mesoscale computational modeling of single and multi track geometry [1, 2]. Coupled with numerical modeling there is also a significant amount of experimental research in high-speed x-ray imaging of the L-PBF process. Existing research has mapped process conditions to single or multi track specimen geometry [3, 4, 5, 6]. This mapping has been done for a limited number of alloys and has hardly, if at all, been conducted with a high level of monitoring data including extensive parameter sweeps. Studying single or multi track level geometry can be used to validate simulation and computational results as well as to evaluate process parameters. Previous studies [7, 8] have included various characterization methods including White Light Interferometry (WLI) and microstructural analysis. The outcome of this type of research is generally a 2D plot mapping process conditions to phenomena such as balling. The dataset presented in this work, however, is significantly richer in completeness and data. This richness will enable research into control schemes that can dynamically improve the stability and reliability of the melt pool process and arguably expand the process window. This data set includes the process parameters, on-axis melt pool monitoring signals, WLI topology scans, and cross sectional images for 352 lines. Most importantly, all these data can be spatially aligned for use in a variety of different research thrusts.

Methodology

A total of 352 AlSi10Mg tracks were produced for this data set. The tracks were melted onto 16 additively manufactured sample blocks. The blocks were produced with 30 µm layers and manufacturer-recommended hatch scan speed of 1550 mm/s, hatch laser power of 360 W, and hatch spacing of 150 µm. The tracks themselves were produced from a 30 µm layer, with a range of process parameters across the domain of laser power of 50-400 W and scan speed of 270-2500 mm/s. Gas flow was also varied for some tracks from 300 to 600 L/min. The specific parameters selected are shown in Fig. 1 and are separated into four groups, which are summarized in Table 1. A Latin hypercube (LHC) sampling method was used to select 28 parameter sets spanning the parameter domain for the gas flow LHC group. These tracks were built on one block each at 300, 400, 500, and 600 L/min gas flow rate, for a total of four blocks. The build parameters group consists of 16 parameter sets selected from the hatch and contour parameters used for larger parts. These 16 parameter sets were also used to produce 4-track pads. The third group of parameters consists of 13 parameter sets that were selected as 'analogous parameters' where the same linear energy density (0.08, 0.16 or 0.24 J/mm) was achieved through three to five combinations of laser power and scan speed. In Fig. 1, these parameters are connected by lines representing their common energy densities. A separate Latin hypercube sampling generated 35 parameter sets to span the full range of laser parameters for the LHC group. The 64 parameter sets from the build parameters, analogous parameters, and LHC groups were built with gas flow of 600 L/min and spread across a total of 12 sample blocks. Each sample block contained 16 single tracks and four 4-track pads. Two copies of each block were built in the middle region of the build plate. One block, which consists mostly of the analogous parameters, was additionally copied to each of the four corners of the build plate to capture potential spatial variations.

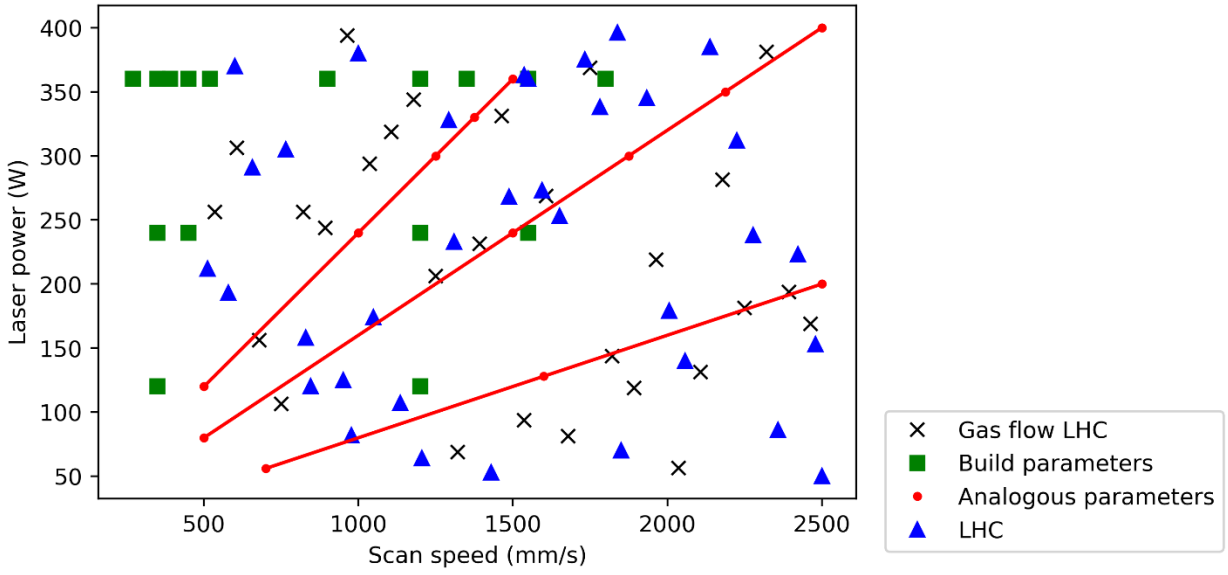

Figure 1. Power-velocity process map showing the 92 different parameter sets used for the tracks, identified by the group to which each set belongs. The analogous parameters are connected by lines representing their common energy densities. The LHC groups were selected by Latin hypercube sampling.

Table 1. Summary of parameter groups.

Parameter group	Number of samples	Laser power range (W)	Scan speed range (mm/s)	Gas flow range (L/min)	Sampling method
Gas flow LHC	28	56.25 – 393.75	536 – 2464	300 – 600	Latin hypercube
Build parameters	16	120 – 360	270 – 1800	600	Hatch and contour parameters from prior builds
Analogous parameters	13	56 – 400	500 – 2500	600	Manually selected
LHC	35	50 – 396	512 – 2500	600	Latin hypercube

A PrintRite3D (Sigma Additive Solutions, formerly Sigma Labs, Santa Fe, United States) melt pool monitoring system was used to collect in-situ build data (MPM data). The system monitors the spectral emission of the melt pool at a sampling rate of up to 200 kHz. It collects data from three photodiodes, representing a high-wavelength signal, a low-wavelength signal, and a wide spectrum signal. This data is processed to produce Thermal Energy Density (TED^{TM}, wide spectrum intensity) and Thermal Emission Planck (TEP^{TM}, ratio of high- and low-wavelength intensities) values. TED and TEP are representative of the total emission from the melt pool and a two color pyrometry measurement calibrated to temperature, respectively [9]. The MPM data for each track was extracted from the whole-build data set.

The surface topology of each track is measured on an Alicona InfiniteFocus system (IFM G4f measurement device) at 10x magnification. Each sample block was imaged individually or in a small group, then sections of the full scan were selected for each track. The resulting images had horizontal resolution of approximately 3.5 μm and vertical resolution of approximately 177 nm. An example of this data for a whole block is shown in Fig. 2a, and for a single track from that block in Fig. 2b.

The cross section images of each track were acquired by cutting and polishing the sample blocks after they were removed from the build plate. Each block was sectioned once, in an arbitrary location roughly in the center of the tracks. The blocks are sectioned on a Stuers Accutom-5 sectioning saw and hot mounted in Polyfast. The samples were polished with a Buehler Automet 250 autopolisher and polished to 0.06 microns with a colloidal silica suspension. The sample thicknesses were measured at each step to enable estimation of the polished plane relative to the topological and MPM data. A Nikon MA200 microscope was used at a magnification of 10x. Images were again collected for an entire block of 20-28 tracks and trimmed to a single image for each track. An example of this cross section is shown in Fig. 2c.

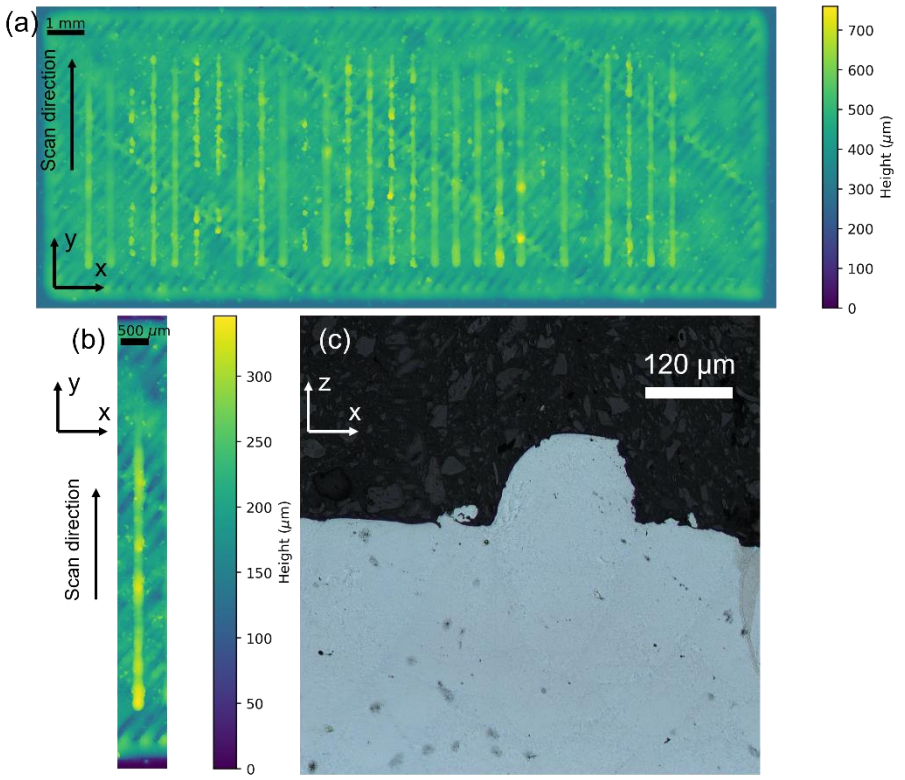

Figure 2. Examples of topology data for (a) a whole block and (b) a single track with the scan direction from the bottom up, with track length of approximately 6 mm, and (c) optical cross section image.

Analysis

The methodologies above created three sets of data for each single track: MPM data, representing both the calibrated temperature measurement and the total emission measurement along with laser location information; the surface topology of the track; and cross section image of the track. The further analysis of these data types was partially automated to expedite analysis. Full automation was not feasible because of the noisy nature of the topology and cross section imaging of single tracks on additively manufactured surfaces, and the wide range of parameters which lead to a variety of track shapes.

Initial processing on the topology data was conducted by manually labeling tracks as either ‘complete’, ‘partial’ or ‘missing’, representing the cases of a coherent track, a broken up or segmented track, or no track, respectively. These cases are demonstrated in Fig. 3. The topology data for each track was independently labeled by four people for a total of five times. Final labels were determined by a majority of the five labels. The start and end positions of each track were manually identified. The cross section images were manually annotated in ImageJ, with the region of the image identified as the track’s cross section marked as white. The cross sections were not etched, therefore the track region was not always clear, depending on polishing and microscope settings. Because of this, not all images could be annotated. Further analysis shown here was limited to single tracks labeled as ‘complete’ and with successful cross section annotations, though valuable information could also be gleaned from the incomplete tracks. A

few additional tracks were removed for various processing issues. This resulted in a total of 156 single tracks down selected for further analysis.

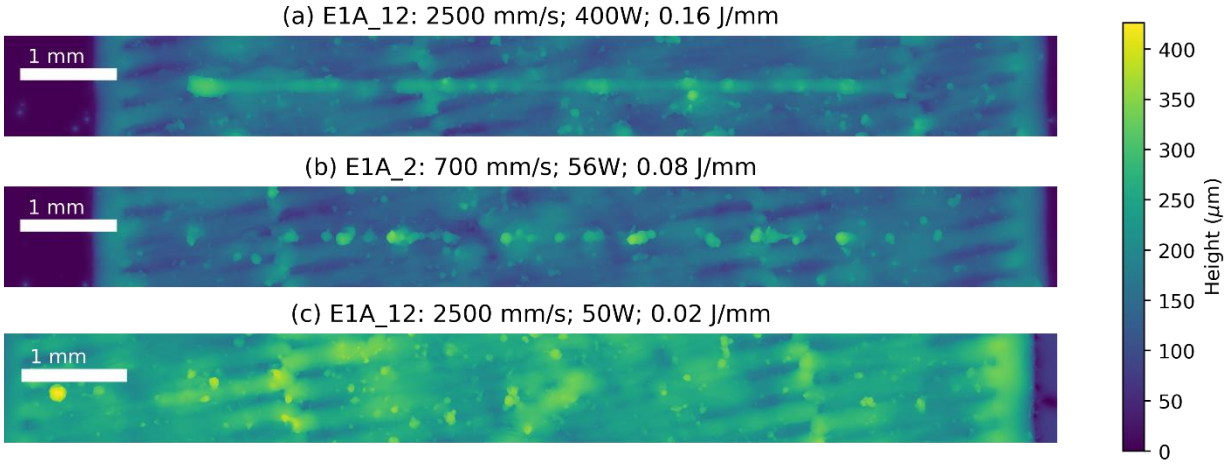

Figure 3. Example topolgy data for (a) complete track, (b) partial track, and (c) missing track. These tracks are approximately 8 mm long.

For the down-selected 156 tracks, the melt pool cross section was analyzed by calculating the dilution and aspect ratios from the annotations. Here, dilution ratio is defined as the ratio between the depth of the track below the level of the substrate and the height of the track above the substrate. Aspect ratio is defined as the ratio between the height of the track above the substrate and the width of the track.

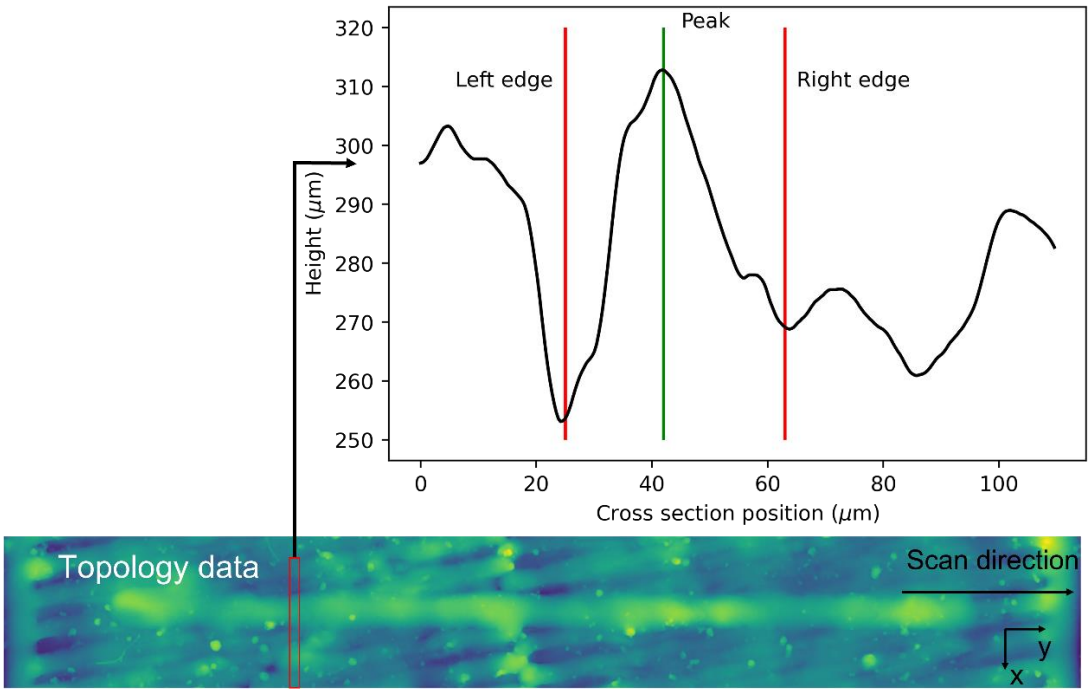

Figure 4. An example of the topology analysis, taking a slice of the topology data perpendicular to the track and extracting the peak, left, and right edge for the slice.

The height and width for the full length of each track was calculated from the topology data. The topology data was sliced perpendicular to the track, and the height, left edge and right edge were extracted for each slice based on the track profile cross section at that point. These points are shown in an example in Fig. 4. The width was then calculated from the difference between the left and right edges. The MPM data, height, and width data were then processed so that each data set had the same spatial resolution along the track. This registration was conducted by generating 1000 y-positions evenly spaced along the track, then selecting the height, width, and MPM data values with y-positions closest to each of the 1000 generated points.

Results

The track cohesion classification of the 352 tracks shows a general trend of both lack of fusion (LOF) and balling defects. In Fig. 5, as the energy density of the tracks decreases, the cohesion of the tracks decreases, shifting from complete track, to incomplete, to absent. Additionally, as the scan speed increases, even with a corresponding increase in laser power, the tracks become less cohesive, demonstrating a balling up effect. Tracks in the balling and LOF regions were excluded from further analysis here because the inconsistent topology of the tracks requires a different processing technique to generate useful information.

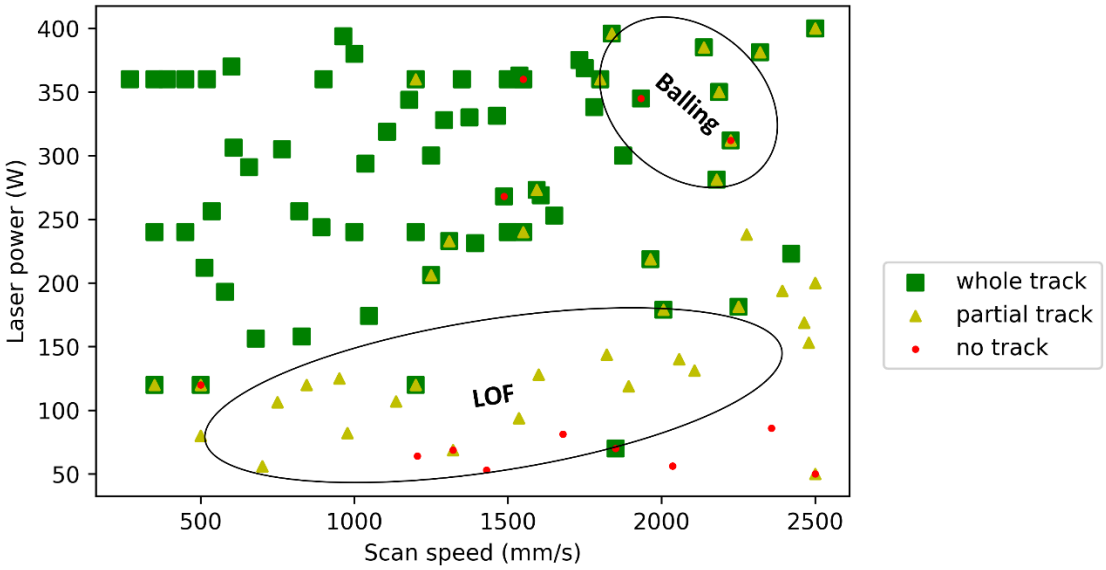

Figure 5. Power-velocity process map showing the cohesion of 352 tracks across 92 parameters. Due to the repetition of parameters across duplicate sample blocks, some parameter sets have multiple labels.

Examination of the topology data with the MPM data along the length of the track shows some correlation. Comparison of the average MPM data values for each track with the cross section data and line cohesion classifications did not demonstrate a clear relationship. The reason for this contrast in results is likely the loss of data resolution through the averaging. Since this averaging is not present with the topology/MPM data comparison, a clearer pattern is able to emerge. Fig. 6(a) shows this pattern for the height of the track and the TED signal. Fig. 6(b)

shows the relationship between the width of the track and the TED signal. For both of these plots, the TED signal was smoothed with a moving average of 10 samples. These plots demonstrate that for some regions of the track, the TED signal and track dimensions appear to be moving in similar patterns. However, when applied to the aggregate data of the 155 single tracks selected for this analysis, there does not appear to be a prevailing statistical correlation between MPM data values and track dimensions. This suggests that the relationship between the MPM data and the track dimensions is more complex. The more complex relationship is consistent with the nature of the differences in the data sets. The track dimensions are related to the thermal gradient and morphology of the melt pool at multiple points in time, while the MPM data is only able to capture some of these characteristics at a single point in time. It is also possible that the MPM data shown here captures only one aspect of the changes in melt pool characteristics that leads to the variations in track dimensions and doesn't capture variation due to, for example, variation in the substrate height.

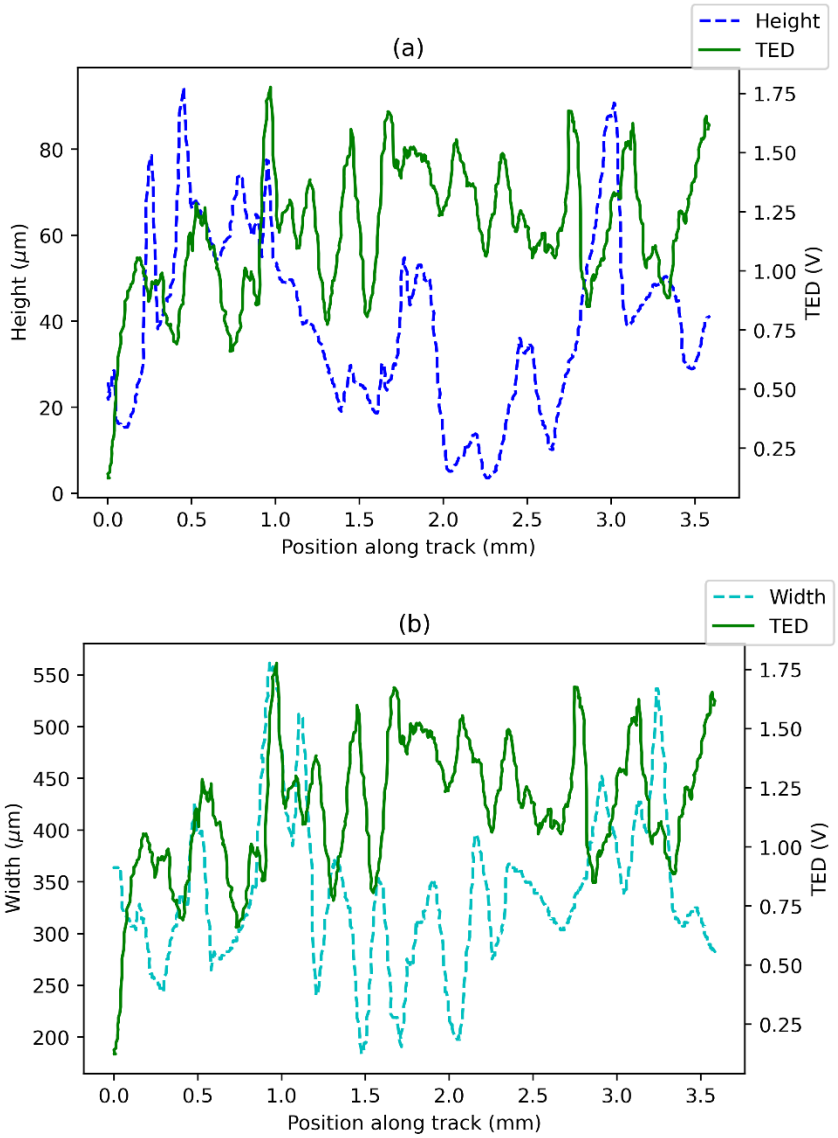

Figure 6. The TED MPM signal and the (a) height and (b) width of the resultant track seem to move in similar patterns for certain sections of the track.

Conclusions and Future Work

Single tracks are the most fundamental component of the L-PBF process. Since L-PBF is an extremely localized manufacturing process, understanding the behavior of single tracks with relation to melt pool monitoring data is crucial to improved process understanding and control. The work presented here demonstrates a framework to generate and analyze large sets of single tracks. The generated data of over 20 GB shows track morphology consistent with expected lack of fusion and balling behavior and illustrates a potential connection between MPM data and resultant track shape. These demonstrations show that the generated data set has the potential to provide useful insights to connect melt pool monitoring to observed track shapes. Further analysis is needed to fully characterize these relationships, including a more robust model to connect complex MPM data behavior to track morphology. Additional analysis of the tracks themselves also includes sample etching, porosity calculations, and analysis of incomplete tracks. The data set generated here is available at: https://github.com/ConorPorter3/Single-Tracks.

Acknowledgements

Research was sponsored by the Army Research Laboratory and was accomplished under Cooperative Agreement Number W911NF-20-2-0292 and W911NF-21-2-02199. The views and conclusions contained in this document are those of the authors and should not be interpreted as representing the official policies, either expressed or implied, of the Army Research Office or the U.S. Government. The U.S. Government is authorized to reproduce and distribute reprints for Government purposes notwithstanding any copyright notation herein.

We appreciate the support from the Northwestern University CHiMaD Metals Processing Facility (CMPF) for providing the additive manufacturing equipment for this work.

This work made use of the MatCI Facility which receives support from the MRSEC Program (NSF DMR-1720139) of the Materials Research Center at Northwestern University.

References

[1] Kumar H, Kumaraguru S, Paul CP, Bindra KS, Faster temperature prediction in the powder bed fusion process through the development of a surrogate model, Optics and Laser Technology, 2021.

[2] Yuan W, Chen H, Li S, Heng Y, Yin S, Wei, Q, Understanding of adopting flat-top laser in laser powder bed fusion processed Inconel 718 alloy: simulation of single-track scanning and experiment, Journal of Materials Research and Technology, 2022.

[3] Laitinen V, Piili H, Nyamekye P, Ullakkoa K, and Salminen A, Effect of process parameters on the formation of single track in pulsed laser powder bed fusion, Procedia Manufacturing, 2019.

[4] Aversa A, Moshiri M, Librera E, Hadi M, Marchese G, Manifredi D, Lorusso M, Calginano F, Biamino S, Lombardi M, Pavese M, Single scan track analyses on aluminium based powders, Journal of Materials Processing Tehcnology, 2018.

[5] Dilip J, Anam A, Pal D, Stucker B, A short study on the fabrication of single track deposits in SLM and characterization, Solid Freeform Fabrication Symposium, 2016.

[6] Gaikwad A, Giera B, Guss G, Forien J, Matthews M, Rao P, Heterogeneous sensing and scientific machine learning for quality assurance in laser powder bed fusion – A single-track study, Additive Manufacturing, 2020.

[7] He Y, Zhonga M, Beuth J, Webler B, A study of microstructure and cracking behavior of H13 tool steel produced by laser powder bed fusion using single-tracks, multi-track pads, and 3D cubes, Journal of Materials Processing Technology, 2020.

[8] Shrestha S, Chou K, A study of transient and steady-state regions from single-track deposition in laser powder bed fusion, Journal of Manufacturing Processes, 2021.

[9] Lane B, Jacquemetton L, Piltch M, Beckett D, Thermal calibration of commercial melt pool monitoring sensors on a laser powder bed fusion system, NIST Advanced Manufacturing Series 100-35, 2020.